

Orbital ordering in LaMnO₃: Electron-lattice versus electron-electron interactions

Wei-Guo Yin,¹ Dmitri Volja,^{1,2} and Wei Ku^{1,2}

¹Physics Department, Brookhaven National Laboratory, Upton, NY 11973

²Physics Department, State University of New York, Stony Brook, NY 11790

(Dated: Received September 2, 2005)

The relative importance of electron-lattice (e-l) and electron-electron (e-e) interactions in ordering orbitals in LaMnO₃ is systematically examined within the LDA+*U* approximation of density functional theory. A realistic effective Hamiltonian is derived from novel Wannier state analysis of the electronic structure. Surprisingly, e-l interaction ($\simeq 0.9$ eV) alone is found insufficient to stabilize the orbital ordered state. On the other hand, e-e interaction ($\simeq 1.7$ eV) not only induces orbital ordering, but also greatly facilitates the Jahn-Teller distortion via enhanced localization. Further experimental means to quantify the competition between these two mechanisms are proposed.

PACS numbers: 75.47.Lx, 71.70.-d, 71.70.Ej, 75.30.Fv

Study of perovskite manganites has been one of the main focuses of recent research in condensed matter physics, not only because of their great potentials in technological applications related to colossal magnetoresistance (CMR) in La_{1-x}Ca_xMnO₃, but also because these strongly correlated electron materials (SCEM) are ideally instrumental to the understanding of the complex interplay of the charge, spin, orbital, and lattice degrees of freedom that leads to abundant fascinating phenomena, including long range order in all the above channels [1].

The unusual orbital degree of freedom in the manganites, which is the focus of our study, originates from the singly occupied degenerate e_g states (d_{z^2} and $d_{x^2-y^2}$) of the Mn³⁺ 3*d* electrons in the high-spin configuration ($t_{2g}^3 e_g^1$) due to the ligand-field splitting and strong Hund's coupling. This orbital degeneracy makes the Mn³⁺ ion Jahn-Teller (JT) active: the degeneracy can be split via biaxial distortion of the surrounding oxygen octahedron.

Currently, one of the critical questions on the manganites is the interplay of electron-lattice (e-l) and e_g electron-electron (e-e) interactions [2, 3, 4, 5, 6, 7, 8]. Indeed, carrier mobility [3] and magnetism [2, 5], both essential to the unresolved mechanism of CMR in the manganites [9, 10, 11, 12], respond to these two interactions in a substantially different manner (despite some other aspects [2] reacting similarly). However, even for the simplest parent compound, LaMnO₃ (which presents prototype orbital order (OO) and strongest JT-distortion in the family), various spectral measurements to date [13, 14, 15, 16, 17, 18] have left two possible mechanisms of the OO in dispute: the cooperative JT e-l effect [19] and the e-e superexchange effect [20]. To our knowledge, there is no clear experimental evidence to support one over the other, due to lack of "signatures" in distinguishing these two mechanisms. This leads to great confusions in the field: for example, whether a new type of elementary excitations called orbiton has been observed in Raman scattering spectroscopy [17, 18], and more generally which interaction dominates localization of the e_g electrons and thus facilitates the CMR effects upon dop-

ing LaMnO₃ [9, 10]. It is thus important and timely to discern the real roles of e-l and e-e interactions.

In this Letter, the electronic structure of the prototype LaMnO₃ is systematically analyzed, aiming to quantify the relative importance of e-e and e-l interactions in ordering the orbitals. A realistic effective Hamiltonian for the low energy e_g states is derived from a novel Wannier function-based scheme for general SCEM, with the key effective e-e interaction $U_{\text{eff}} \simeq 1.7$ eV, JT splitting $\Delta_{\text{JT}} \simeq 0.9$ eV, and octahedral-tilting induced tetragonal crystal field $E_z \simeq 0.12$ eV. Surprisingly, e-l interaction alone is found insufficient to stabilize OO. On the other hand, e-e interaction not only induces OO, but also greatly facilitates the JT distortion by strongly localizing the electrons. The present results provide new insight into OO in LaMnO₃, and place stringent constraints on any realistic theories of excitations and CMR in the manganites. Furthermore, our analysis indicates certain *competition* between mechanisms, allowing *direct* experimental determination of their relative strengths.

Aiming at a careful determination of the relevant mechanisms without assuming a particular dominant interaction, the following novel three-step scheme designed for general SCEM is employed, with each step leading to additional insights into essential interactions and more accurate evaluation of their strengths: (i) A systematic analysis of the electronic structure within the LDA+*U* method [22, 23] against various constraints (e.g.: lattice distortion), giving a rough estimate of the relevant e-l and e-e effects; (ii) Construction of the low-energy Wannier states [14, 21], leading to signatures of competition between e-l and e-e interactions, additional tetragonal field effects, and a local representation of the LDA+*U* Hamiltonian, $H^{\text{LDA}+U}$; (iii) Determination of the effective many-body Hamiltonian via a self-consistent mapping to $H^{\text{LDA}+U}$, providing a quantitative evaluation of the interactions and deep microscopic insights.

(i) *Analysis of the LDA+U results.* The results of our systematic study of the electronic structure of LaMnO₃ are summarized in Fig. 1, where the total energy gain per

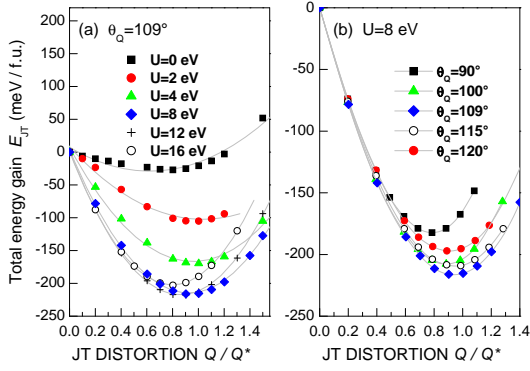


FIG. 1: Total energy gain per formula unit via JT distortion of the MnO_6 octahedra, expressed in $\mathbf{Q}_i \equiv (Q_i^z, Q_i^x) = (\sqrt{2}(l-s), \sqrt{2/3}(2m-l-s))$, with l , m , and s being the long, medium, and short Mn-O bond lengths, respectively. For cooperative JT distortions in LaMnO_3 , $\mathbf{Q}_i = (Q \cos \theta_Q, e^{i\mathbf{q}\cdot\mathbf{R}_i} Q \sin \theta_Q)$ at the i -th Mn site located at \mathbf{R}_i ; in low-temperature phases, $Q = Q^* \equiv 0.4 \text{ \AA}$, $\theta_Q = \theta_Q^* \equiv 109^\circ$, and $\mathbf{q} = (\pi, \pi, 0)$ [27].

formula unit (f.u.), E_{JT} , as a function of cooperative JT distortion vectors \mathbf{Q}_i (defined in the caption) is shown for a wide range of U [23, 24]. Notice that for realistic $U = 8 \text{ eV}$, the crystal structure is stabilized at $Q^* = 0.4 \text{ \AA}$ [Fig. 1(a)] and $\theta_Q^* = 109^\circ$ [Fig. 1(b)], in excellent agreement with experiments [27], supporting the good quality of the LDA+ U approximation for this system.

Surprisingly, e-l interaction alone is found *insufficient* to stabilize the orbital ordered insulating phase: for $U = 0 \text{ eV}$, the system stabilizes in a metallic state at $Q = 0.8Q^*$ with small $E_{\text{JT}} = -27 \text{ meV}$, despite being weakly insulating at $Q = Q^*$ with a small gap of 0.1 eV [28]. On the other hand, E_{JT} dramatically increases in magnitude to -215 meV as U increases to 8 eV , indicating that *the electron localization induced by the e-e interaction greatly facilitates the JT instability*—in fact, OO can be stabilized even without JT distortion [22]. Indeed, as shown in Fig. 1(a), fitting the data points to the JT picture ($E_{\text{JT}} \simeq -\frac{1}{2}gQ + \frac{1}{2}KQ^2$ [19]) is excellent for $U > 4 \text{ eV}$ but unsatisfactory for small U , suggesting that only with $U > 4 \text{ eV}$ the e_g electrons are well localized as assumed in the JT picture. For realistic $U = 8 \text{ eV}$, the JT splitting ($\sim 4E_{\text{JT}}$ at Q^*) is thus $\Delta_{\text{JT}} \sim 0.9 \text{ eV}$, comparable to $\sim 0.8 \text{ eV}$ extrapolated from spectral ellipsometry [15, 16].

It is extremely important to distinguish carefully the JT distortion from other lattice distortions, namely octahedral tilting and its associated octahedral distortion of GdFeO_3 -type. The latter is found negligible in LaMnO_3 , as our study of LaFeO_3 (a JT-inactive counterpart of LaMnO_3 [26]) produces negligible octahedral distortion with total energy gain of merely -3 meV . In contrast, octahedral tilting is found to give large energy gain of -403 meV/f.u. Clearly, a correct assessment of E_{JT} should exclude such a JT-distortion-unrelated contribu-

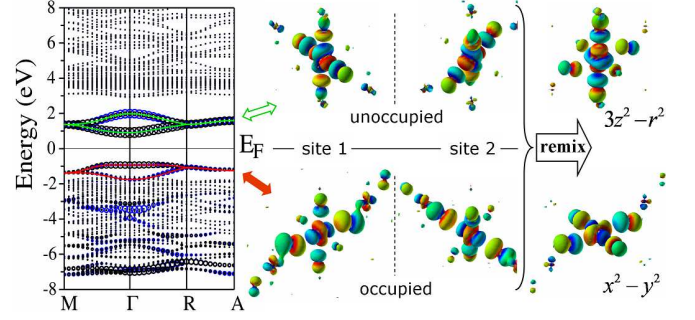


FIG. 2: Left panel: LDA+ U (8 eV) band structure of LaMnO_3 in the real crystal structure, with circles reflecting the weights of the Mn d_{z^2} (black) and $d_{x^2-y^2}$ (blue) symmetries. $M=(\pi, 0, 0)$, $\Gamma=(0, 0, 0)$, $R=(\pi/2, \pi/2, \pi/2)$, and $A=(\pi, 0, \pi/2)$. Solid green and red lines show the dispersions of OO-relevant spin-majority e_g Wannier states, illustrated in right panels (see text).

tion. Therefore, our systematic study was performed with the experimental octahedral tilting angle ($\phi_{\text{tilt}}=16^\circ$, nearly unchanged upon JT distortion [26, 27]).

In addition to localizing e_g states, e-e interaction plays other crucial roles, as clearly demonstrated in the LDA+ U (8 eV) band structure (Fig. 2, left panel): The $\sim 2.6 \text{ eV}$ splitting between the spin-majority occupied and unoccupied e_g bands near the Fermi energy is too large to be accounted for with the estimated JT splitting ($\sim 0.9 \text{ eV}$), indicating an effective on-site repulsion $U_{\text{eff}} \sim 1.7 \text{ eV}$. Note that the U_{eff} relevant to OO is to be distinguished from the “bare” U acting between atomic Mn $3d$ states, as U_{eff} acts only between the low-energy e_g Wannier states (WSs, discussed below), and thus includes effects of additional screening and slight delocalization via hybridization that weaken the “bare” repulsion. Also note that the considerable amount of e_g -character near the bottom of the oxygen $2p$ bands ($[-8, -6] \text{ eV}$) is not very relevant to OO, as such feature has its origin in strong hybridization with the oxygen $2p$ orbitals, independent of ordering of the orbitals. Though it does imply the charge-transfer nature of the manganites in general.

(ii) *Construction of WSs.* To proceed with more quantitative evaluation of the above effects and to identify other relevant mechanisms, a well-defined local (Wannier) representation of the *low-energy* e_g states is necessary for further theoretical formulation. To this end, our previously developed energy-resolved symmetry-specific WS construction [14, 21] is extended to allow mixed symmetry with a constraint search for maximal localization [29]. The resulting orbital ordered occupied ($[-2.5, 0] \text{ eV}$) and unoccupied WSs ($[0, 2.5] \text{ eV}$) are illustrated in Fig. 2 (middle panel), from which the staggered ordering of the orbitals is apparent, as well as the considerable weight at the oxygen sites due to strong p - d hybridization. Also given in Fig. 2 are band dispersions (solid lines) corresponding to these WSs, obtained by diagonalizing the

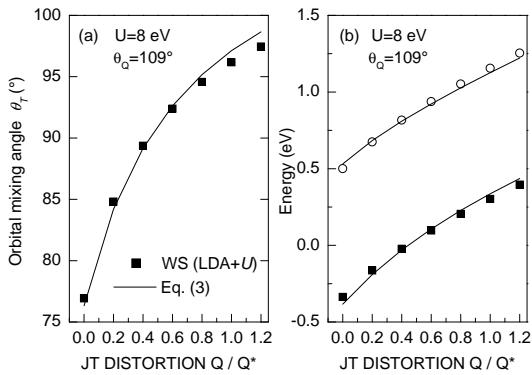


FIG. 3: (a) θ_T as a function of JT distortion. (b) Comparison of results from Eq. (3) (lines) and LDA+U: $H_{i\uparrow,i\uparrow}^{LDA+U}$ – $H_{i\downarrow,i\downarrow}^{LDA+U}$ (squares) and $H_{i\uparrow,i\downarrow}^{LDA+U}$ (circles).

LDA+U Hamiltonian in Wannier representation,

$$H_{jm',im}^{LDA+U} = \langle jm' | H^{LDA+U} | im \rangle, \quad (1)$$

where $|im\rangle$ denote the m -th WS at site i . For convenient theoretical formulation, a second set of WSs with pure $d_{3z^2-r^2}$ and $d_{x^2-y^2}$ symmetries are built from unitary transformation (‘remixing’, c.f. Fig. 2) of the first set of WSs. The resulting ‘conventional’ WSs form a realistic basis for our theoretical modeling below.

An important observation emerges from the occupied WSs in Fig. 2: They do not possess the $d_{3z^2-r^2}$ and $d_{3y^2-r^2}$ symmetry expected from the JT picture [19]. Indeed, the occupied states $|occ.\rangle = \cos\frac{\theta_T}{2}|3z^2-r^2\rangle \pm \sin\frac{\theta_T}{2}|x^2-y^2\rangle$ do not follow $\theta_T = \theta_Q = 120^\circ$ from the JT model [19]. As it will become more apparent with the realistic Hamiltonian below, while e-e and e-l interactions induce cooperatively the staggered OO in this system, different mechanisms actually compete in determining the ‘orbital mixing angle’, θ_T . Specifically, the purely electronic (superexchange) mechanism [20] favors $\theta_T = 90^\circ$ for the cubic perovskite structure [3, 4], which was confirmed by our LDA+U calculations (not shown). This competition makes θ_T a *sensitive measure* of the relative importance of leading mechanisms for OO.

An additional relevant mechanism can now be clearly observed from Fig. 3(a), in which θ_T , evaluated from the above transformation between the above two sets of WSs, is plotted against various magnitude of JT distortion Q with experimental θ_Q . In the absence of the JT effect ($Q = 0$), $\theta_T = 76^\circ$ is much smaller than 90° expected from the superexchange effect [3, 4]. This reflects the importance of the tetragonal crystal field, E_z , yielded mainly from the octahedral-titling in the real structure [4], as E_z favors $\theta_T = 0^\circ$ instead. Notice also from Fig. 3(a) that θ_T grows as Q increases, reflecting a sizeable e-l interaction. Nevertheless, even at optimal (experimental) Q , θ_T is still way below θ_Q , confirming that the JT effect is far from being dominant.

(iii) *Mapping the Effective Hamiltonian.* Based on the above systematic analysis, the concrete physics of the low-energy spin-majority e_g states can be described by an effective Hamiltonian including U_{eff} , Δ_{JT} , and E_z :

$$H^{\text{eff}} = \sum_{\langle ij \rangle \gamma \gamma'} t_{ij}^{\gamma \gamma'} d_{j\gamma'}^\dagger d_{i\gamma} + U_{\text{eff}} \sum_i n_{i\uparrow} n_{i\downarrow} - g \sum_i \mathbf{T}_i \cdot \mathbf{Q}_i - E_z \sum_i T_i^z + K(Q), \quad (2)$$

where γ and γ' refer to the conventional WSs, denoting $|\uparrow\rangle = |3z^2-r^2\rangle$ and $|\downarrow\rangle = |y^2-x^2\rangle$. $\mathbf{T}_i = (T_i^z, T_i^x)$ with $T_i^z = (d_{i\uparrow}^\dagger d_{i\uparrow} - d_{i\downarrow}^\dagger d_{i\downarrow})/2$ and $T_i^x = (d_{i\uparrow}^\dagger d_{i\downarrow} + d_{i\downarrow}^\dagger d_{i\uparrow})/2$ are pseudo-spin operators. The in-plane nearest neighbor hopping integrals are $t_{ij}^{\uparrow\uparrow} = 3t/4$, $t_{ij}^{\downarrow\downarrow} = t/4$, and $t_{ij}^{\uparrow\downarrow} = t_{ij}^{\downarrow\uparrow} = \mp\sqrt{3}t/4$ (the \mp sign distinguishes hopping along the x and y directions), while out-of-plane hoppings are strongly suppressed in the A-type antiferromagnetic ground state due to the double-exchange effect [2, 3, 4]. g is the JT coupling constant and $K(Q) = \frac{k}{2} \sum_i \mathbf{Q}_i \cdot \mathbf{Q}_i + \dots$ consists of lattice energies.

To properly map out these parameters from the LDA+U results, an unambiguous approach is developed in this study. Employing the fact that strong local e-e interaction is approximated in LDA+U in an effective HF manner [22], a proper connection can be made on the same WS basis by matching $H_{j\gamma',i\gamma}^{LDA+U}$ with the *self-consistent* HF expression of H^{eff} :

$$\sum_{\langle ij \rangle \gamma \gamma'} t_{ij}^{\gamma \gamma'} d_{j\gamma'}^\dagger d_{i\gamma} - \sum_i \mathbf{T}_i \cdot \mathbf{B}_i + E_0. \quad (3)$$

Here the effective field $\mathbf{B}_i = (B_i^z, B_i^x)$, where $B_i^z = 2U_{\text{eff}}\langle T_i^z \rangle + E_z + gQ_i^z$ and $B_i^x = 2U_{\text{eff}}\langle T_i^x \rangle + gQ_i^x$. $\langle T_i^z \rangle = T^z$ and $\langle T_i^x \rangle = e^{i\mathbf{q} \cdot \mathbf{R}_i} T^x$ with $\mathbf{q} = (\pi, \pi, 0)$ are the components of the ‘pseudo-spin density wave’ mean field $\langle \mathbf{T}_i \rangle$, which must be determined self-consistently and is *not* necessarily parallel to \mathbf{Q}_i . $E_0 = K(Q) + U_{\text{eff}}|\langle \mathbf{T}_i \rangle|^2 + U_{\text{eff}}/4$. As shown in Fig. 3, an excellent mapping results from $t = -0.6$ eV, $U_{\text{eff}} = 1.72$ eV, $\Delta_{\text{JT}} = gQ^* = 0.87$ eV, and $E_z = 0.12$ eV. Remarkably, even $\theta_T = \tan^{-1} T^x/T^z$ obtained from the effective Hamiltonian also agrees well with the LDA+U results. That is, the effective Hamiltonian accurately reproduce not only all the LDA+U energies, but also the wavefunctions.

Further insight into the relative importance of e-e and e-l interactions now can be obtained by examining the contribution of each term of the effective Hamiltonian, Eq. (2), to the HF total energy, as shown in Table I. First, consider Δ_0 (first row), the energy gain purely due to the OO formation (finite $\langle \mathbf{T}_i \rangle$) in the absence of JT distortion. Consistent with the above LDA+U results, e-e interaction alone (-173 meV) overwhelms the kinetic energy cost (132 meV) and induces OO with the total energy gain of -50 meV. More intriguingly, the additional energy gain via cooperative JT distortion \mathbf{Q}^* , referred to

TABLE I: Contribution of the energy terms in Eq. (2) to Δ_0 and Δ_{Q^*} (see text), in unit of meV per formula unit.

	Total	U_{eff}	g	K	E_z	t
Δ_0	-50	-173	0	0	-9	132
Δ_{Q^*}	-215	-129	-356	96	16	158

as Δ_{Q^*} (second row), consists of considerable further contribution from e-e interaction (-129 meV). Without the e-e interaction, the JT coupling (-356 meV) alone is insufficient to overcome the energy cost of lattice (96 meV) and kinetic (290 meV) energy. That is, e-e interaction, whose contribution is enhanced due to increased $\langle \mathbf{T}_i \rangle$, serves as a *hidden driving force* for octahedral distortion. Overall, U_{eff} is more important to OO in LaMnO₃ than the JT coupling, while their effects on cooperative octahedral distortion are comparable.

The present results place stringent constraints on any realistic theories of the manganites and interpretations of their excitation spectra, for example, current controversy on the recently observed 120 – 160 meV Raman shifts of incident photons resonant at $E_{\text{res}} \simeq 2$ eV [17, 18]. On the one hand, the excitations were interpreted as orbital waves, or ‘orbitons’, derived from the pseudo-spin superexchange model in the large U_{eff} limit of Eq. (2) [20]. With the orbiton spectrum gap $\sim 2.5J_{\text{orb}} + \Delta_{\text{JT}}$ [3, 4, 30] and superexchange coupling constant $J_{\text{orb}} \simeq 40 - 50$ meV ($\propto t^2/U_{\text{eff}}$), this scenario requires small $\Delta_{\text{JT}} \leq 50$ meV [7, 18, 30]. On the other hand, in the JT scenario the Raman shifts were attributed to two-phonon processes (single phonon frequency $\sim 60 - 80$ meV) induced by a phonon assisted *on-site* $d_i^4 \rightarrow d_i^4$ transition, requiring large $\Delta_{\text{JT}} \simeq E_{\text{res}} \simeq 2$ eV [17, 31]. In contrast, our quantitative results ($\Delta_{\text{JT}} \simeq 0.9$ eV and $U_{\text{eff}} \simeq 1.7$ eV) show that the spin-majority e_g states are in the intermediate e-e interaction regime with comparable JT coupling. Thus, a more reasonable picture would be two-phonon processes mediated by optically active *inter-site* $d_i^4 d_j^4 \rightarrow d_i^3 d_j^5$ transition with $E_{\text{res}} \simeq 2$ eV [14, 15]. *Direct experimental verification* of our results includes probing, e.g., on-site d - d transition (~ 0.9 eV) via inelastic X-ray scattering, or θ_T via nuclear magnetic resonance.

In summary, we have quantified the relative importance of e-e and e-l interactions in ordering orbitals in LaMnO₃ using a new theoretical approach. A realistic effective Hamiltonian resulting from this quantitative method reproduces consistently both LDA+ U energies and wavefunctions. Intermediate e-e interaction ($U_{\text{eff}} \simeq 1.7$ eV) is found to play a crucial role in inducing OO and localizing the electrons, which in turn enhances the JT interaction ($\Delta_{\text{JT}} \simeq 0.9$ eV) and stabilizes JT distortion. Furthermore, a clear “signature” of competition between e-e and e-l interactions is given via the orbital mixing angle $\theta_T < \theta_Q$. Experimental means to directly clarify the relative strengths of the leading mechanisms

are suggested. The developed general theoretical scheme can be applied to other strongly correlated materials.

We are grateful to P. Allen, E. Dagotto, S. Grenier, J. Hill, A.J. Millis, A. Moreo, G. Sawatzky, D. Singh, and J. Thomas for helpful discussions. W.Y. thanks M. Lufaso and P. Woodward for providing SPuDS [26] and T. Chatterji for providing structural data [27]. Brookhaven National Laboratory is supported by U.S. Department of Energy under Contract No. DE-AC02-98CH1-886. This work is partially supported by DOE-CMSN.

-
- [1] E. Dagotto, *Nanoscale Phase Separation and Colossal Magnetoresistance* (Springer Series in Solid State Sciences vol. 136, Springer, 2003).
 - [2] T. Hotta, A. L. Malvezzi, and E. Dagotto, Phys. Rev. B **62**, 9432 (2000).
 - [3] W.-G. Yin, H. Q. Lin, and C. D. Gong, Phys. Rev. Lett. **87**, 047204 (2001).
 - [4] J. Bala and A. M. Oleś, Phys. Rev. B **62**, R6085 (2000).
 - [5] M. V. Mostovoy and D. I. Khomskii, Phys. Rev. Lett. **92**, 167201 (2004).
 - [6] K. H. Ahn and A. J. Millis, Phys. Rev. B **61**, 13545 (2000).
 - [7] S. Okamoto, S. Ishihara, and S. Maekawa, Phys. Rev. B **65**, 144403 (2002).
 - [8] R. Tyer, W. M. Temmerman, Z. Szotek, G. Banach, A. Svane, L. Petit, and G. A. Gehring, Europhys. Lett. **65**, 519 (2004).
 - [9] A. J. Millis, Nature (London) **392**, 147 (1998).
 - [10] C. M. Varma, Phys. Rev. B **54**, 7328 (1996).
 - [11] A. S. Alexandrov, and A. M. Bratkovsky, Phys. Rev. Lett. **84**, 2043 (2000).
 - [12] T. V. Ramakrishnan, H. R. Krishnamurthy, S. R. Hassan, and G. Venkateswara Pai, Phys. Rev. Lett. **92**, 157203 (2004).
 - [13] Y. Murakami, J. P. Hill, D. Gibbs, M. Blume, I. Koyama, M. Tanaka, H. Kawata, T. Arima, Y. Tokura, K. Hirota, et al., Phys. Rev. Lett. **81**, 582 (1998).
 - [14] S. Grenier, J. P. Hill, V. Kiryukhin, W. Ku, Y.-J. Kim, K. J. Thomas, S.-W. Cheong, Y. Tokura, Y. Tomioka, D. Casa, et al., Phys. Rev. Lett. **94**, 047203 (2005).
 - [15] N. N. Kovaleva, A. V. Boris, C. Bernhard, A. Kulkakov, A. Pimenov, A. M. Balbashov, G. Khaliullin, and B. Keimer, Phys. Rev. Lett. **93**, 147204 (2004).
 - [16] R. Rauer, M. Rübhausen, and K. Dörr, to be published.
 - [17] R. Krüger, B. Schulz, S. Naler, R. Rauer, D. Budelmann, J. Bäckström, K. H. Kim, S.-W. Cheong, V. Perebeinos, and M. Rübhausen, Phys. Rev. Lett. **92**, 097203 (2004).
 - [18] E. Saitoh, S. Okamoto, K. T. Takahashi, K. Tobe, K. Yamamoto, T. Kimura, S. Ishihara, S. Maekawa, and Y. Tokura, Nature (London) **410**, 180 (2001).
 - [19] J. Kanamori, J. Appl. Phys. **31**, 14S (1960).
 - [20] K. Kugel and D. Khomskii, Sov. Phys. JETP **37**, 725 (1973).
 - [21] W. Ku, H. Rosner, W. E. Pickett, and R. T. Scalettar, Phys. Rev. Lett. **89**, 167204 (2002).
 - [22] V. I. Anisimov, F. Aryasetiawan, and A. I. Lichtenstein, J. Phys.: Condens. Matter **9**, 767 (1997).
 - [23] LDA+ U ($U=8$ eV, $J=0.11U$) was shown to appropriately

- describe the $(\pi, \pi, 0)$ orbital and $(0, 0, \pi)$ magnetic structures of LaMnO_3 , see I. S. Elfimov and V. I. Anisimov and G. A. Sawatzky, Phys. Rev. Lett. **82**, 4264 (1999).
- [24] All our LDA+ U results were obtained with the linearized augmented plane wave method [25] for the A-type antiferromagnetic phase with experimental volume and fixed $J=0.11U$. Hypothetic crystal structures were prepared with SPuDS [26].
- [25] P. Blaha *et al.*, Comput. Phys. Commun. **147**, 71 (2002).
- [26] M. W. Lufaso and P. M. Woodward, Acta Cryst. B **60**, 10 (2004).
- [27] T. Chatterji, F. Fauth, B. Ouladdiaf, P. Mandal, and B. Ghosh, Phys. Rev. B **68**, 052406 (2003).
- [28] W. E. Pickett and D. J. Singh, Phys. Rev. B **53**, 1146 (1996).
- [29] W. Ku *et al.*, to be published.
- [30] J. van den Brink, Phys. Rev. Lett. **87**, 217202 (2001).
- [31] P. B. Allen and V. Perebeinos, Phys. Rev. Lett. **83**, 4828 (1999).